Development of the wide IF 230 GHz SIS mixer for KVN-Pyeongchang VLBI station

Naeun Shin [1,2], Jung-Won Lee [*,2], and Ming-Jye Wang [3]

***Abstract*—A 230 GHz SIS mixer is designed for the new Korean VLBI Network (KVN) telescope in Pyeongchang, South Korea. The design is focused on a good performance in the IF frequency range of 4-16 GHz over the RF band from 211 to 275 GHz. The designed mixer has series-connected junctions, and two tuning circuits are introduced. Type A uses transmission lines between the probe and the junction array to match the junction embedding impedance to the optimum source impedance. Type B uses junctions as a tuning element in transmission lines to replace the highly capacitive strip lines which increase capacitance from the tuning circuit. The capacitance of the whole circuits, required to be minimized for wider IF bandwidth, is 190 fF and 210 fF respectively. In the simulation, over the whole RF band, two designs show single sideband receiver noise temperatures less than two times the quantum limit, and the receiver temperatures vary less than 5 K within IF frequency from 4 to 16 GHz.**

***Index Terms*—receiver, SIS mixer, submillimeter**

I. Introduction

THE Korean VLBI Network (KVN) comprises three stations operating four receiver bands from 22 to 129 GHz. In addition to the current telescopes, the fourth telescope which is operable up to 230 GHz is being constructed in Pyeongchang, located in the eastern part of South Korea.

Through the recent outstanding works of the Event Horizon Telescope (EHT), the importance of the 230 GHz receiver is highlighted [1]. Optical depth at 230 GHz is about 0.3 (T_{sys} = around 200 K) in the cold winter season at Seoul. We expect similar atmospheric conditions at KVN-Pyeongchang station. The planned facility receivers of the new telescope are composed of a compact tri-band receiver (CTR) receiving 22/43/86 GHz [2] and 150/230 GHz receivers.

IF instantaneous bandwidth of KVN was just 2 GHz for all frontends in the beginning, constrained mainly by the processing bandwidth of the VLBI backends available around 2010. With the advent of a wide-band digitizer and data recorders working up to 32 Gbps, the mixers must be upgraded to provide a wider IF bandwidth of 16 GHz. At 230 GHz frequency, SIS mixers are still more sensitive than HEMT amplifiers and such requirement for wide IF bandwidth is the main motivation of this development.

In this paper, we present two wide IF bandwidth designs for KVN 230 GHz SIS mixers focusing on low noise performance at an IF frequency range of 4-16 GHz over the RF frequency from 211 to 275 GHz. A dominant factor that limits the IF bandwidth of an SIS mixer is often the RC time constant of the IF circuit in a mixer [4]. Although the lower normal resistance, R_N less than 10 ohms of a high Jc junction giving source impedance of several R_N at IF frequency helps for wide bandwidth by simpler matching to a following LNA, we adhere to normal Nb-Al/AlOx-Nb junctions for this development. It is because lowering capacitance at the IF frequency range using tri-layer-based junctions is another effective way to widen bandwidth by avoiding mixer gain roll-off.

An SIS mixer is generally composed of an RF tuning circuit to load optimum embedding impedance to a junction or junction array and an RF choke for transmission of IF signal. Therefore, limiting the total capacitance of such elements as an RF tuning network, RF choke, and junctions at the IF frequency range is required to achieve wider IF bandwidth. In our design, we utilized series-connected junctions for the lower total geometrical capacitance which still affects on a signal at the IF frequency range. We focused on lowering the capacitance of the RF tuning circuit and RF choke while increasing other mixer performances. In order to calculate the capacitance and the noise temperature, RF/IF circuit simulations were progressed using Supermix[5][6], a software package for the simulation of SIS mixers. The two types of circuits for the mixers are described in the following sections.

TABLE I
Parameters used for the probe design

substrate material	quartz
waveguide size (μm)	940 x 470
probe radius (μm)	00
probe height (μm)	100
probe angle (degree)	45
substrate thickness (μm)	100
air gap height above substrate (μm)	50
air gap height below substrate (μm)	100
probe impedance (μm)	75 + 0.1 Ω

II. Mixer Designs

A. Probe

The size of the input waveguide is chosen as WR3.7 to cover the RF frequency range from 211 to 275 GHz. We adopted a single-sided probe [7] which has an RF choke at one side. The RF signal is transferred to the channel as shown in Figure 1. A channel where the substrate is located is perpendicular

[1] Department of Physics and Astronomy, Seoul National University, Gwanak-ro 1, Gwanak-gu, Seoul 08826, Republic of Korea
[2] Korea Astronomy and Space science Institute, Daedeok-daero 776, Yuseong-gu, Daejeon 34055, Republic of Korea
[3] Academia Sinica Institute of Astronomy and Astrophysics, 11F of AS/NTU Astronomy-Mathematics Building, No.1, Sec. 4, Roosevelt Rd, Taipei 10617, Taiwan
Corresponding author: J.-W. Lee (email: jwl@kasi.re.kr).

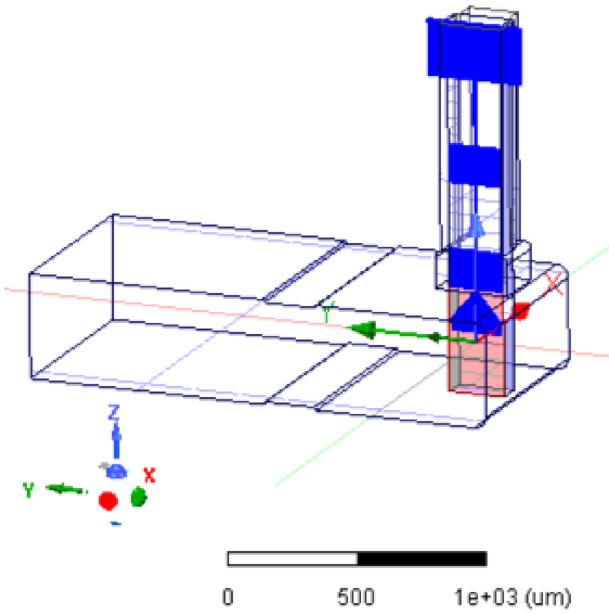

Fig. 1. A transition from a full height waveguide to probe simulated in HFSS. The substrate is extending out of the input waveguide and the thin-film microstrip circuit including junctions is patterned on the substrate. The probe has a home-plate shape; a combination of an isosceles triangle and a rectangle. In Table I, the length of two identical sides of the triangle is denoted as a probe radius, and the angle between them stands for a probe angle. A height of a rectangle is expressed as a probe height.

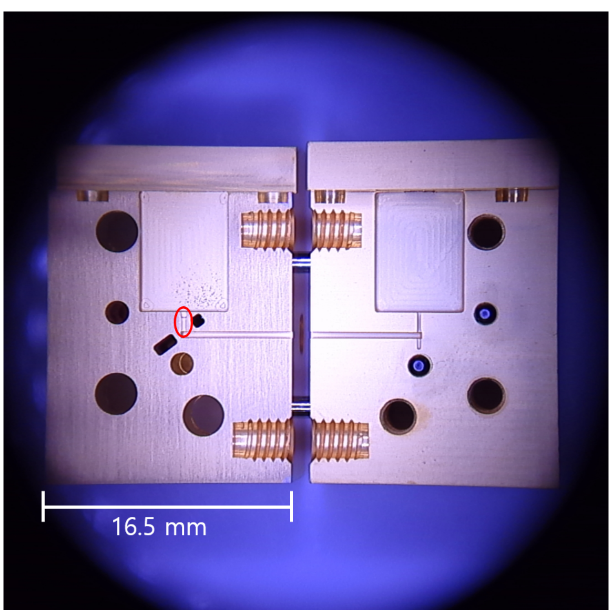

Fig. 2. Photo of the top and the bottom block of the mixer block (from left to right). The WR3.7 input waveguide is seen at the center. The mixer chip will be placed in the red-circled slot.

to the axis of the propagation in the waveguide. SIS junctions integrated with a superconducting tuning circuit and an RF choke are laid on a quartz substrate. We optimized a feed point impedance using Ansys HFSS, the 3D EM simulator. Several structures in the mixer block were used to optimize the feed point impedance having a compact and symmetric tear-drop impedance trace on the Smith chart as shown in Figure 3. This method facilitates providing proper embedding impedance for junctions over the RF frequency range. First, the home-plate shape probe has more extra tuning parameters than the radial probe. The optimized parameters of the home plate probe are listed in Table I. In addition, widening the substrate channel under the first section of the RF choke decreases the imaginary component of the probe impedance. There are capacitive tuning steps on the long sides of the input waveguide near the probe reducing the height of the waveguide by 5%. Those structures decrease influences by non-propagating modes and return loss. At last, an air gap is added under the substrate to increase the cutoff frequency of the dielectric-loaded channel. As a result, the feed point impedance is 73+j0.1 Ω on average with a small variance. This probe impedance is shown in Figure 3. The mixer block containing the waveguide probe had been fabricated as seen in Figure 2. It will be combined with the mixer chip which consists of junctions, tuning elements, and an RF choke.

TABLE II
JUNCTION PARAMETERS

area (μm^2)	1.1 $\times$ 1.1
number of junctions	3
normal resistance (Ω)	26
fractional bandwidth	0.26
specific capacitance, C_s (fF/μm^2)	80
critical current density, J_c (A/cm^2)	6700

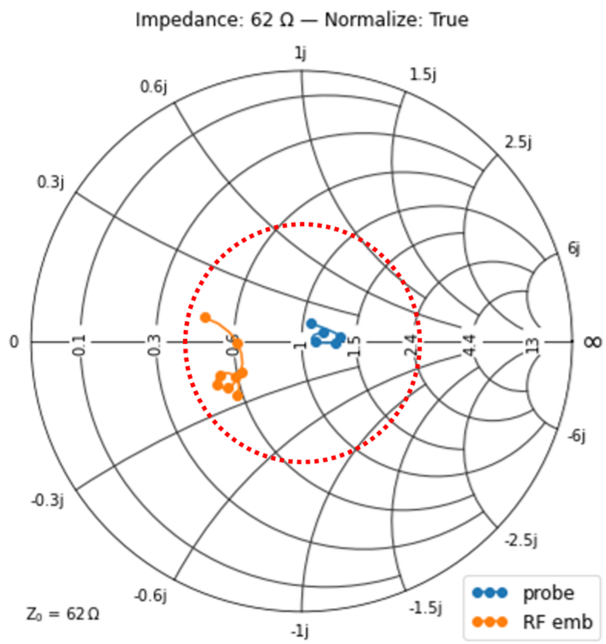

Fig. 3. The power from the feed point is transferred to the junction through tuning elements and it is finally seen to the junction as an RF embedding impedance. The RF embedding impedance of the Type 1 circuit from RF 211 to 275 GHz is located inside of the $|\rho| = 0.4$ circle indicated as a red dashed line. The Smith chart is normalized with an optimum source impedance.

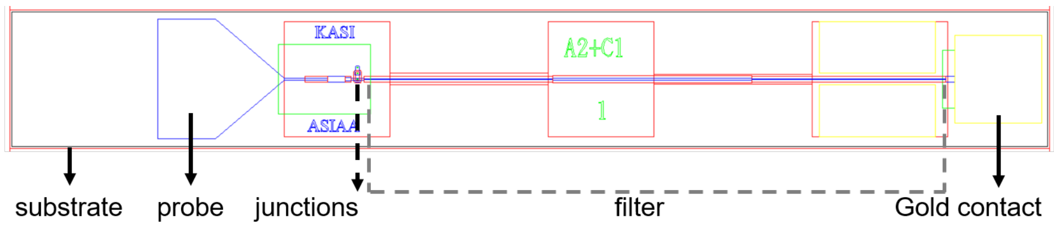

Fig. 4. The configuration of the mixer chip. The layers are denoted in different colors and the number in the center is information about the circuit and the number of columns on the wafer. The largest rectangle on the edge is a substrate. The probe at the left is a connection between the waveguide to the thin-film microstrip. The bonding pad is located at the last section of the RF choke followed by a gold contact. The gray dotted line is indicating a range of the RF filter composed of CPWs.

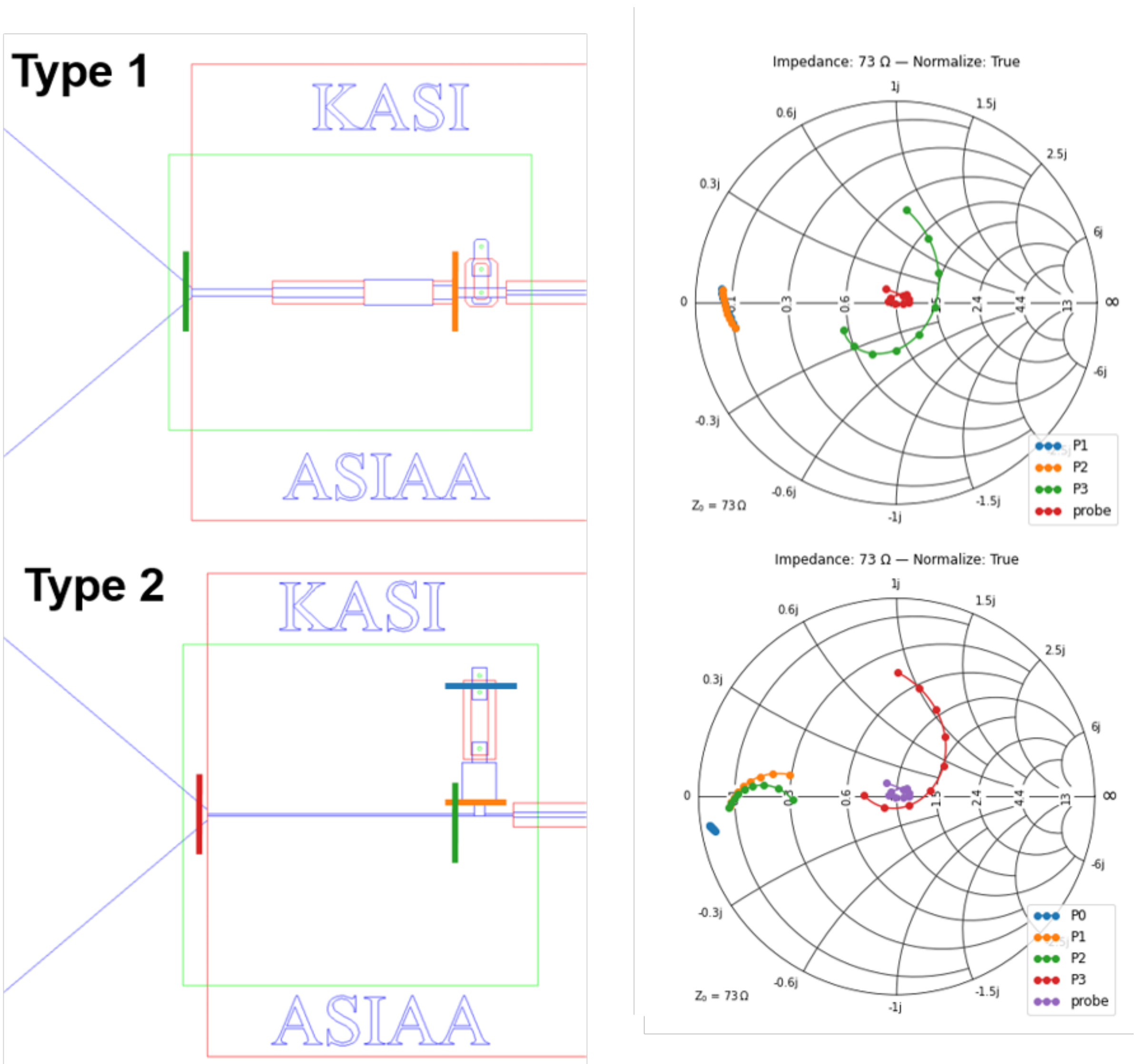

Fig. 5. (Top) An enlarged view of the Type 1 circuit between the probe and an island where the junctions are located. Thick lines are indicating the respective planes where the impedances are obtained. We can see the impedance is matched to the probe impedance from P1 to P3 through tuning elements. (Bottom) A maximized view of a Type 2 circuit showing an impedance matching from P0 to P3 through microstrips and CPWs.

B. Junctions and tuning circuits

The series-connected array of three Nb-Al/AlOx-Nb junctions is used in designs. The required critical current density is about 7000 $\mathrm{A/cm^2}$, estimated from the parameters in Table II. Two of the three junctions are placed on an island structure, as seen in Figure 4 and Figure 5, which is expected to have small series inductance to the capacitive junctions. To simulate the performance of the elements in the mixer chip, we used a program named Supermix, which performs harmonic balance for large signal analysis and small signal analysis based on Tucker's quantum mixer theory. The RF tuning elements composed of microstrips and coplanar waveguides (CPW) tune out the residual capacitance of the junction array.

There have been two approaches regarding junctions in a tuning circuit: that considers a junction as a lumped element as a whole [8] or an element used in distributed circuit[4]. Since the noise and conversion gain of the SIS mixer depends on the embedding impedance seen by the junction [8], the first approach focused on locating the embedding impedance nearby the optimum source impedance using only external transmission lines. The optimum source impedance is calculated by the Ke and Feldman formula based on the Tucker theory [3] and the boundary of the advantageous operating region is $|\rho| = 0.4$ where the $|\rho|$ is the reflection coefficient from the optimum source impedance. The RF source impedance combined with junction capacitance of Type 1 is shown in Figure 3, and it is well positioned near the optimum source impedance in RF bandwidth.

While the first one assumed the junction array essentially as a lumped junction, the second approach handled a junction as a series or shunt element in a transmission line. In this way, a low impedance tuning transmission line section that has a larger capacitance can be replaced with a junction partially tuned with a series inductive line and a less capacitive shunt line. In effect, the junction itself can be re-used as low impedance matching elements and the total capacitance of the junctions can be reduced in series connection [4].

After the tuning network and junctions, an RF choke composed of multiple CPWs follows, working as cascaded quarter-wave transformers. It is identical in two designs. We used scikit-rf, a Python package for linear RF circuit analysis, to calculate impedance transformation by the CPWs of the RF choke. The effective lengths of physical lines for the determined impedances are calculated using the package and implemented in the codes in Supermix. We confirmed most of the local oscillator (LO) power is transmitted to junctions and blocked by the RF choke from the simulation in Supermix. The additional surface impedance of a superconducting conductor is also taken into account.

As shown in Fig 5, both designs show coupled impedances with the feed point impedance in the RF bandwidth. Although the couplings are not fully optimized, it was the most enhanced result to match the impedance in the low and high frequencies at the same time with low capacitance tuning elements. The coupling can be advanced in the future with the improved design.

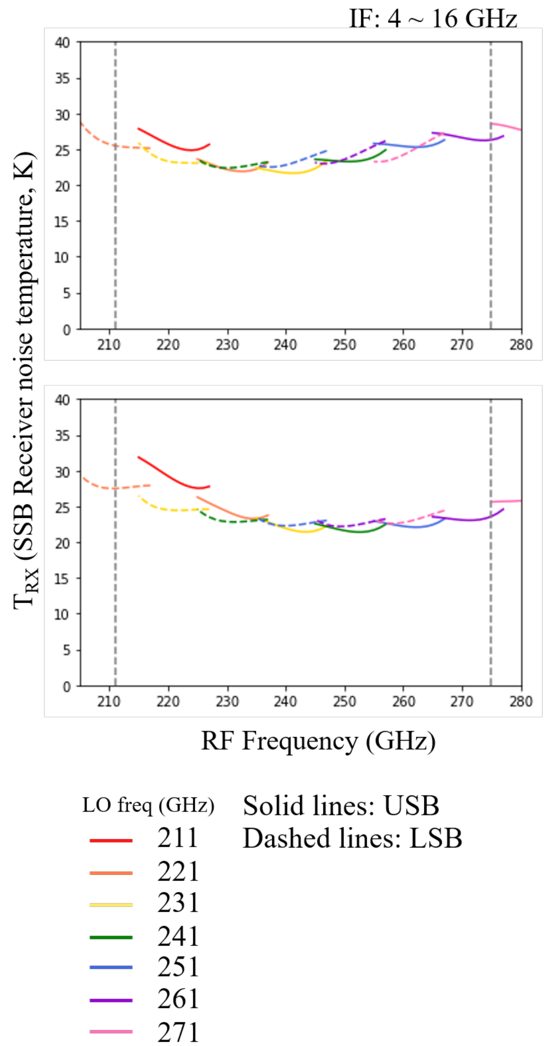

Fig. 6. The performance of designs simulated in Supermix. The top is for Type 1 and the bottom is about Type 2. $\mathrm{T_{rx}}$ is an SSB noise temperature and is calculated using a gain and a mixer noise temperature. Solid lines denoted upper sideband (USB) receiver noise temperatures with specific LO frequencies from 211 to 271 GHz and dashed lines are for lower sidebands (LSB).

III. Simulated Performance

A. Results from Supermix

The total capacitance of the circuit is critical to the IF bandwidth. We estimate the capacitance of the whole circuit by measuring the admittance at the IF output port using Supermix. Type A and B shows a total capacitance of 190 fF, and 210 fF, respectively, and these are compatible with previous 230 GHz mixers, which generally show capacitances value larger than 200 fF[9]. Two designs are expected to have an IF bandwidth of up to 16 GHz. For IF frequency range from 4 to 16 GHz, Type A and B show single sideband (SSB) mixer receiver noise temperatures less than two times the quantum limit, and $\mathrm{T_{rx}}$ varies less than 5 K throughout the RF frequency range from 211 to 275 GHz. Type A shows less variation in the receiver temperature than Type B in the whole RF band. Type B has flatter sensitivity in the IF band with a given LO frequency than type A except for LO at 211 GHz.

B. Analysis of the IF embedding impedance

The USB receiver noise temperature reaches the lowest point around IF frequency 14 GHz and increases a few K in other frequencies in case of LO 241 GHz as Figure 6 shows. The elevation of the noise temperature is originated from the decrease of the mixer gain at IF band edges. Since this trend appears in two types of RF tuning circuits at the same time, analysis of the IF circuit can explain the variance of the mixer gain. In general, optimizing the IF load admittance is required to obtain approximately constant mixer gain in wide IF bandwidth [10]. IF embedding impedance of 10 times R_N usually shows maximum gain, though the number can be different depending on LO and IF frequencies [11]. Roughly, the mixer conversion gain varies primarily with the real impedance and is affected less by changes in the imaginary impedance of the IF embedding circuit. As Figure 7 presents, the behavior of IF embedding impedance can be a reason for the gain variance. It will be confirmed after the lab test of the mixer chips which is under fabrication.

IV. Conclusion

We introduce designs of the wide IF bandwidth 230 GHz SIS mixer for the 4th KVN telescope under construction at Pyeongchang, South Korea. Covering the RF band of 211-275 GHz, the probe was optimized to get close to constant impedance. Two tuning circuits were designed to show similar noise temperature performance at the IF frequency range from 4 to 16 GHz. The mixer block has been made successfully, and we expect to have lab tests of the fabricated mixer chips in the near future.

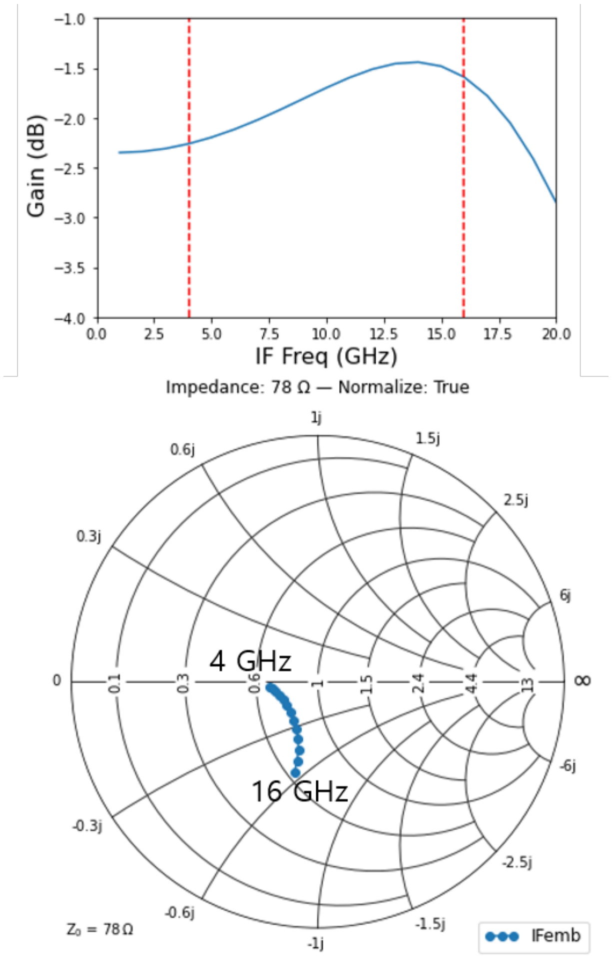

Fig. 7. The gain curve and IF embedding impedance of Type 1 from IF frequency 4 to 16 GHz with LO 243 GHz, which is normalized to 3 times of R_n. The gain curve has a peak at 14 GHz and the IF embedding impedance has the largest real part at the same point. It replies that the change of the gain is mainly contributed by the matching between the if impedance of the junction and the real part of the if embedding impedance.

References

[1] The Event Horizon Telescope collaboration et al., "First M87 Event Horizon Telescope Results. I. The Shadow of the Supermassive Black Hole", *ApJ*, 875, L1, 2019.

[2] Han, et al., A millimeter-wave quasi-optical circuit for compact triple-band receiving system. Journal of Infrared, Millimeter, and Terahertz Waves, September 2017.

[3] Ke and Feldman, "Optimum source conductance for high frequency superconducting quasiparticle receivers", *IEEE Trans. Microw. Theory Techn*, Apr. 1993.

[4] Tong, et al., "Wideband SIS receivers Using Series Distributed SIS Junction Array", *Proc. 29th IEEE International Symposium on Space THz Technology*, March 2018.

[5] Ward, et al., "Supermix: a Flexible Software Library for High-Frequency Circuit Simulation, including SIS Mixers and Superconducting Components", *Proc. 10th Int. Symposium on Space Terahertz Technology*, March 1999.

[6] Rice et al., "Fast Harmonic Balance of SIS Mixers with Multiple Junctions and Superconducting Circuits", *Proc. of 10th International Symposium on Space Terahertz Technology*, March 1999.

[7] Kooi et al., "A 275-425 GHz Tunerless Waveguide Receiver Based on AlN-barrier SIS Technology", *IEEE Transactions on microwave theory and techniques*, October 2017.

[8] Kerr, et al., "Development of the ALMA Band-3 and Band-6 Sideband-Separating SIS Mixers", *IEEE Transactions on Terahertz science and technology*, March 2014.

[9] Kerr et al., "MMA memo 205: A tunerless SIS mixer for 200-280 GHz with low output capacitance and inductance", *Proc. of 9th International Symposium on Space Terahertz Technology*, March 1998.

[10] Kooi et al., "Regarding the IF output conductance of SIS tunnel junctions and the integration with cryogenic InP MMIC amplifiers", *Proc. of 10th International Symposium on Space Terahertz Technology*, March 1999.

[11] Rice et al., "SIS Mixer Design for a Broadband Millimeter Spectrometer Suitable for Rapid Line Surveys and Redshift Determinations", *Proc of SPIE - The International Society for Optical Engineering*, November 2004.